VOLUME 8, NUMBER 4, APRIL 2008



NANO LETTERS

# The Function of a $TiO_2$ Compact Layer in Dye-Sensitized Solar Cells Incorporating "Planar" Organic Dyes

**Anthony Burke,*,† Seigo Ito,† Henry Snaith,† Udo Bach,‡ Joe Kwiatkowski,§ and Michael Grätzel†**

*Laboratory for Photonics and Interfaces, Institute of Chemical Sciences and Engineering, Ecole Polytechnique Fédérale de Lausanne, Station 6, CH-1015 Lausanne, Switzerland, ARC Australian Centre for Electromaterials Science, Monash University, Victoria 3800, Australia, and Department of Physics, Imperial College London, London SW7 2BW, England*

*Received July 3, 2007; Revised Manuscript Received February 11, 2008*

**ABSTRACT**

**We present a device based study into the operation of liquid electrolyte dye-sensitized solar cells (DSSC's) using organic dyes. We find that, for these systems, it is entirely necessary to employ a compact $TiO_2$ layer between the transparent fluorine doped $SnO_2$ (FTO) anode and the electrolyte in order to reduce charge recombination losses. By incorporation of a compact layer, the device efficiency can be increased by over 160% under simulated full sun illumination and more than doubled at lower light intensities. This is strong evidence that the more widely employed ruthenium based sensitizers act as to "insulate" the anode against recombination losses and that many planar organic dyes employed in DSSC's could greatly benefit from the use of a compact $TiO_2$ blocking layer. This is in strong contrast to DSSC's sensitized with ruthenium based systems, where the introduction of compact $TiO_2$ has only marginal effects on conversion efficiencies.**

The limited availability of ruthenium as a raw material and the demand driven increase in the cost of ruthenium based dyes could become a serious issue for commercialization of DSSC's in the future.[1,2] Lately, organic dyes have received much attention with respect to their application in DSSC's[3–5] due to their low cost of production and their environmentally friendly nature in comparison to their ruthenium based metal–ligand counter parts. We have tested a series of organic dyes in DSSC's and the effect of interfacial charge recombination at the FTO surface has been studied. We find that the solar cell efficiency can be significantly increased if a compact $TiO_2$ layer is deposited onto the FTO glass substrate before the application of the mesoporous nanocrystalline $TiO_2$ layer. This is in strong contrast to recent work by Ito et al.,[6] who have shown that in the case of the sensitizer bis-tetrabutylammonium *cis*-dithiocyanato-*N*,*N*′-bis-2,2′-bipyridine-4-carboxylic acid, 4′ -carboxylate ruthenium(II), N719, only a small suppression of the surface charge

* Corresponding author. E-mail: anthony.burke@eng.monash.edu.au.
† Laboratory for Photonics and Interfaces, Institute of Chemical Sciences and Engineering, Ecole Polytechnique Fédérale de Lausanne.
‡ ARC Australian Centre for Electromaterials Science, Monash University.
§ Department of Physics, Imperial College London.

10.1021/nl071588b CCC: $40.75 
**Published on Web 03/05/2008**

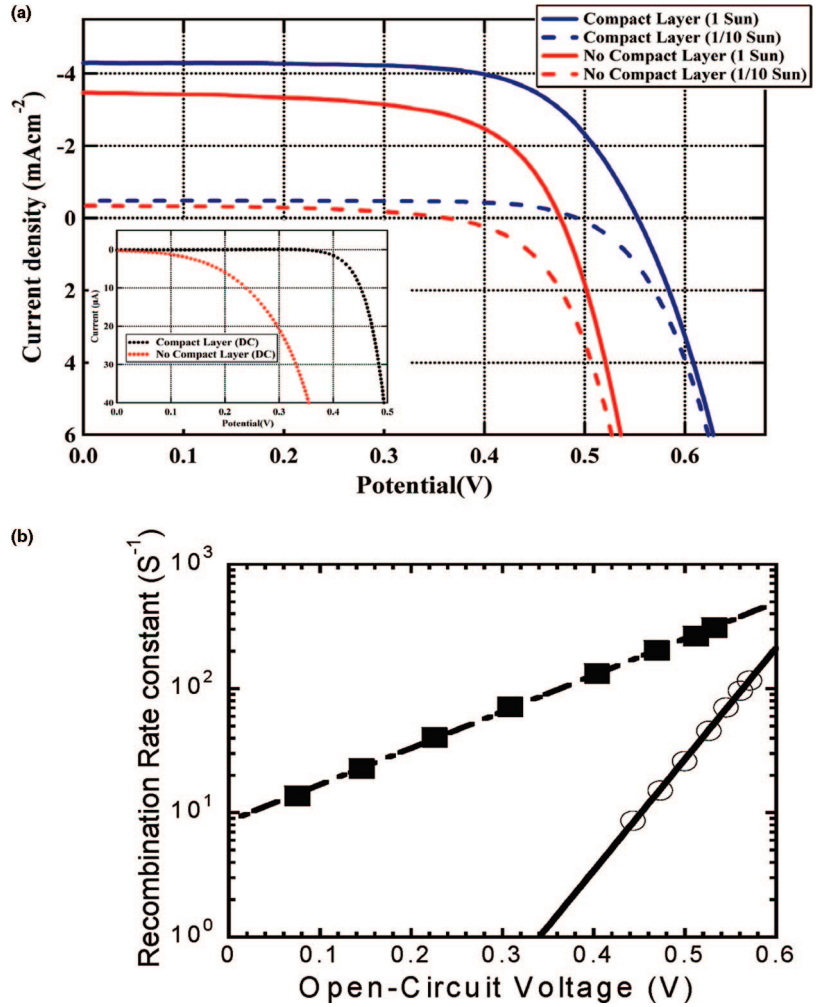


**Figure 1.** (a) *IV* curves of two cells both in the presence (blue) and absence (red) of a compact $TiO_2$ blocking layer on the FTO. The thick lines and dashed lines represent the performance at 1 Sun and 1/10 Sun, respectively. The inset shows the dark currents with (black) and without (red) the compact layer. (b) Charge recombination rate constant derived from transient open-circuit voltage decay measurements for a DSSC with a blocking layer (open circles, solid line) and without a blocking layer (solid squares, dot−dashed line).

recombination was seen with the compact layers. This suggests that the dye itself essentially screens the electrons in the FTO from the iodine species in the electrolyte. In the case of the standard ruthenium dyes, ab initio calculations have shown that the highest occupied molecular orbital (HOMO level) is actually shared by both the ruthenium metal center and the isothiocyanate (NCS) ligands, indicating that the positive charge is distributed between the metal center and the NCS ligands.[7] Because of the large size of the ruthenium complex and the fact that the bis-2,2′-bipyridine-4-carboxylic acid moiety interacts strongly with the FTO surface, a physical separation of the injected electrons and the $I_3^-$ in the electrolyte is obtained. Here, the distance appears to play a critical role in the probability of electron transfer from the FTO to the electrolyte.

The devices were fabricated by following a similar method to Ito et al. The nanoporous $TiO_2$ films were composed of a 6 $\mu$m film of 20 nm nanoparticles and 4 $\mu$m film of 400 nm light scattering particles. Films are generally treated with $TiCl_4$, which is advantageous for device performance. We do not employ it here, as we want to study a clean system without the added complication of a thin $TiO_2$ layer formed by this treatment.

Figure 1a shows the current–voltage ($I-V$) curves of two typical DSSCs sensitized with (4*E*)-4-{[3-(2-carboxyethyl)-1,1-dimethyl-1*H*-benzo[*e*]indolium-2-yl]methylene}-2-{(*E*)-[3-(2-carboxyethyl)-1,1-dimethyl-1,3-dihydro-2*H*-benzo[*e*]indol-2-ylidene]methyl}-3-oxocyclobut-1-en-1-olate triethylammonium salt[8] (termed B1, see Figure 3) with and without a compact $TiO_2$ blocking layer. It is clear that the cells without a compact layer perform incredibly poorly at low light levels and there is a significant increase in open-circuit voltage for the cells with a blocking layer. At 1 Sun (simulated AM1.5, 100 mW $cm^{-2}$) the large increases in the fill factor (FF), current, and potential give efficiencies of ~1.6% with the incorporation of a blocking layer, whereas the cells without a compact layer only attained efficiencies of 1.0%. This difference is further exaggerated at low light levels where an increase in efficiency from 0.6 to 1.6% at 1/10 Sun was seen. This equates to a dramatic increase in efficiency of 160% and 230% at 1 Sun and 1/10 Sun, respectively. The dark current–voltage curves for devices

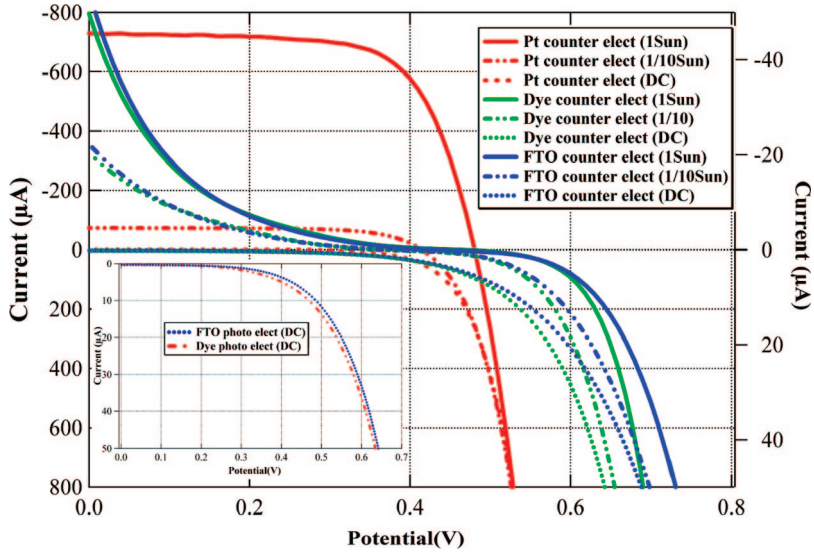


**Figure 2.** Comparison of devices incorporating a B1 dye-sensitized $TiO_2$ working electrode (WE) and utilizing a standard platinized FTO CE (red), a dye catalyzed CE (green), and a bare FTO CE as control (blue). The inset compares the dark currents (DC's) of bare (blue) and a dye-covered (red) FTO WE, both fabricated with a standard platinized CE. The left-hand axis corresponds to the device containing the standard Pt-coated CE and the right-hand axis corresponds to the devices containing the bare FTO and B1-coated FTO counter electrodes.

with and without a compact layer are presented in the inset to Figure 1a. There is a much earlier dark current onset for the devices with no compact layer, demonstrating enhanced back electron transfer from the anode to the electrolyte. Because of the slower kinetics at the bare FTO (as compared to the platinum), the rate at the counter electrode (CE) is higher and so only a small reduction in the photocurrent is seen at short circuit. As will be discussed later, this is confirmed in the independent IPCE measurements of similar systems and explains the difference in the short circuit currents seen at 1 Sun. This is also in excellent agreement with the theoretical model presented by Ferber et al.,[9] who showed that if the recombination rate is reduced, an increase in both current and potential at $I_{sc}$ and $V_{oc}$, respectively, will be seen. The above device results may be therefore simply explained by a reduced parallel "shunt" resistance in the photovoltaic circuit.[10] To further investigate the severity of this effect, we look at how the charge recombination lifetime varies between the two devices.

We have performed transient open-circuit voltage decay measurements by a similar method to O'Regan et al.[11] (Figure 1b). Here, a white light bias was generated from an array of diodes (Lumiled model LXHL-NWE8 whitestar) with red light pulsed diodes (LXHL-ND98 redstar, 0.2 s square pulse width, 100 ns rise and fall time) as the perturbation source controlled by a fast solid-state switch. The voltage dynamics were recorded on a PC-interfaced Keithley 2400 source meter with a 500 $\mu$s response time. The perturbation light source was set to a suitably low level that the voltage decay kinetics were monoexponential. By varying the white light bias intensity, we could estimate the lifetime of the electrons over a range of cell potentials. The results are presented in Figure 1b.

We observe that, in the presence of the compact $TiO_2$ layer, the charge recombination rate constant is phenomenally reduced. For example, at a cell voltage of 450 mV, the charge recombination is more than 1 order of magnitude faster for the device with no blocking layer. As the surface of nanocrystalline $TiO_2$ on the electrode is approximately $1 \times 10^3$ times greater than that of the FTO,[12] this suggests that the rate of reaction at the FTO surface is many orders of magnitude faster than at the $TiO_2$. Here, the only difference in the layers is the presence or absence of the compact blocking layer. For two parallel recombination processes, the rate equation should take the following form $k_{rec} = k_{FTO} + k_{TiO_2}$, where $k_{FTO}$ is the recombination rate constant at the FTO and $k_{TiO_2}$ at the $TiO_2$ nanoparticle interface. We would expect $k_{FTO}$ to be approximately zero in the presence of the blocking layer and less variant to "voltage" because the material can be considered metallic. However, for $TiO_2$, the electron density increases exponentially as the voltage increases, resulting in an exponential increase in $k_{TiO_2}$ with voltage. This is likely to be the reason why the two curves converge with increasing voltage because $k_{TiO_2}$ becomes the dominating recombination pathway.

Furthermore, we note that $k_{FTO}$ is the rate of electron transfer from the FTO to the oxidized species in the electrolyte. This will be enhanced if the holes are in close proximity to the FTO surface. As mentioned, dye layers located at the FTO−electrolyte interface can potentially *decrease* interfacial recombination by forming a spacer layer that separates FTO and oxidized species in the electrolyte or *increase* recombination by acting as a catalyst to promote the two-electron reduction step from triiodide ($I_3^-$) to iodide ($I^-$). To investigate which of those two effects is responsible for the fundamentally different behavior between N719 and B1 sensitized solar cells, dark current–voltage measurements of closed cells composed of a bare FTO electrode both in the presence and absence of B1 were carried out (Figure 2inset). The presence of the dye bound to the surface of the FTO was confirmed via UV–vis spectroscopy.

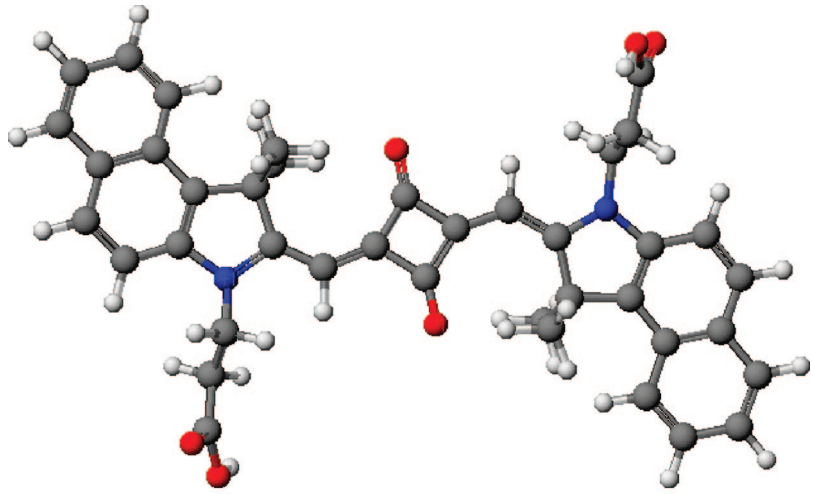

**Figure 3.** PM3 geometry optimized structure of B1 in the acid form. The *x* and *y* axes run along the breadth and length of the molecule, respectively, with the *z* axis extending out of the plane of the page.

Both the final cells and the control FTO plates were studied and the characteristic spectrum for B1 attached to the surface of $TiO_2$ was seen. This not only confirms that the dye was present but that it was also chemisorbed to the surface of the FTO.

In the inset to Figure 2, we can see that there is a slight shift in the onset of the dark current in the cells containing a thin layer of B1 dye in comparison to those with plain FTO. Two explanations are thus possible. The first and most likely is that the pH of the surface has decreased due to an increased number of protons from the dye solution. This proton effect has been seen for the dye N719 and was reported by Nazeeruddin et al.[13] Alternatively, the dye may have a catalytic effect drawing the $I_3^-$ ions closer to the surface and thereby increasing the rate of recombination with electrons from the FTO. To confirm whether the latter is indeed possible, a series of B1 sensitized cells incorporating a blocking layer were made and the CE varied. Here, a comparison of the standard cells utilizing platinum, bare FTO, as a control and FTO with dye adsorbed on the surface of the electrodes, was made (Figure 2). We emphasize that here we are using the dye-coated FTO substrate as the CE in place of the standard platinum-coated CE.

Because the dark currents are similar and there is no significant difference between the photovoltaic performances of the B1 sensitized FTO and FTO control CE, we concluded that the dye does not function as a catalyst. The "S-shaped" nature of these curves is characteristic of a large series resistance, which likely arises from the relatively poor electron injection from FTO when compared to the platinum usually employed. Ruling out the catalytic effect, the slight shift in dark current onset for cells under normal working conditions (Figure 2 inset), with and without dye, is attributed to increased proton concentration at the surface of the electrode.[13]

To explain the increased recombination at the FTO interface, it is instructive to consider the size and orientation of the dye on the surface. The majority of organic dyes consist of highly conjugated systems, suggesting that the molecules are generally planar with SP2 hybridization. In good agreement with the PM3 optimized structure (Figure 3), ground-state optimization results for a very similar dye to B1 have also shown that the quasi-trans or $C_{2h}$ structure is favored.[14] Furthermore, crystallographic data from Kobayashi et al. has confirmed the $C_{2h}$ structure for the dye calculated above.[15] On the FTO, the dyes can either lie flat, i.e., *z* axis parallel to the surface normal (Figure 3), slanted, i.e., *x* axis parallel to surface normal or perpendicular to it, with the *y* axis parallel to the surface normal. To understand the adsorption properties of the dye, nanoporous dye-sensitized $TiO_2$ films were studied. These can be readily measured and characterized by FTIR spectroscopy. Here, both the pure dye in the acid form and the dye adsorbed on the surface of the $TiO_2$ were compared. The free carboxylic acid peak, which is found at 1734 $cm^{-1}$, disappears upon adsorption on the $TiO_2$. To test if the same holds true for the solar cell devices, the FTIR experiment was repeated, but this time the standard dipping solution used in solar cell fabrication (containing both chenodeoxycholic acid and *t*-butylpyridine) was employed. The layers were subsequently post-treated with a pH 3 solution of hydrochloric acid to ensure that any free carboxylic acid groups would be protonated and thus visible in the IR-spectrum. The spectra for dye adsorbed on $TiO_2$ were identical before and after the acid treatment. Therefore, we can conclude that the dye attaches through a bidentate coordination mode to the surface. From this, we can thus eliminate the following situations: (1) the dye attaches with the *y* axis parallel to the surface normal in either the cis or trans conformations, (2) the dye attaches with the *x* axis parallel to the surface normal in the trans form, because these would all result in one unbound carboxyl group. We therefore conclude that the dye adsorbs with either the *x* or *z* axes parallel to the surface normal as the cis or trans conformations, respectively. Though the evidence strongly suggests that the dye exists in the trans configuration, we cannot entirely rule out the possibility that the dye adsorbs in the cis confirmation. We estimate that if

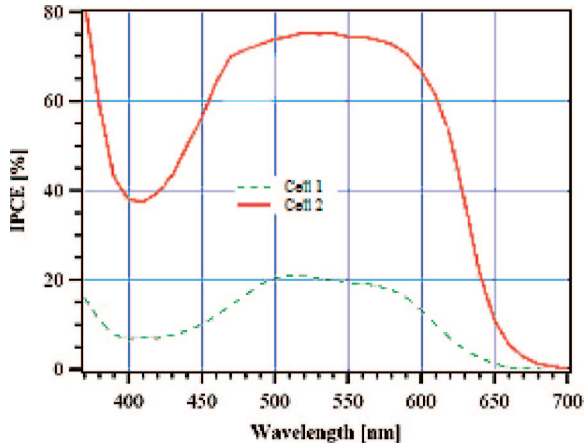


**Figure 4.** Example of an IPCE of two solar cells sensitized with a merocyanine dye (Mc2, see Supporting Information.). The cell incorporating a blocking layer is shown as cell 2 (red line).

the dye lies with the *x* axis parallel to the surface normal, the maximum separation distance will be less than 0.7 nm. If the dye rests with the *z* axis parallel to the surface normal, however, the monolayer separation between FTO and electrolyte will be reduced still further. In both instances, the separation of the electrolyte from the FTO surface is considerably less than that seen for N719.[16] It therefore appears reasonable to postulate that the overall dye monolayer thickness will influence the recombination kinetics across the FTO/dye/electrolyte interface.

Thus, we suggest that bulky organic dyes having a less planar structure and possibly an attaching group along the long axis of the molecule will be beneficial by reducing the dark current losses at the FTO interface. An organic dye that incidentally possesses all these characteristics is the indolene dye D149 from Uchida.[4] This dye has been shown by Ito et al. to function well even in the absence of a compact layer.[17]

One final demonstration of the importance of blocking layers is shown in Figure 4. Here a series of dyes was tested in solar cells where a high incident photon-to-electron conversion efficiency (IPCE) value was required. It was seen that in the absence of a compact layer, IPCE values of around 10–20% were obtained. Upon the addition of such a layer, the light-harvesting efficiencies were more than tripled. Again these dyes were similar to the squaraine dye B1 used here. The data and information on the dyes has been included in the Supporting Information.

In conclusion, the importance of a blocking layer in organic dye-sensitized solar cells has been demonstrated. This work suggests that organic dyes behave in a fundamentally different manner to that of N719 and those with a more bulky structure and less planarity may function more effectively as sensitizers in DSSC's. In addition, we conclude that the proximity of the $I_3^-$ from the FTO surface is related to the dyes orientation and structure and therefore has a direct effect on cell efficiency. The screening of novel dyes for their potential application in DSSC's is often achieved through the direct fabrication of solar cells. Many new organic dyes, however, may well be overlooked as they do not perform well in the absence of a blocking layer. The work is important to those searching for viable organic alternatives to the ruthenium based systems, which has both economic and environmental implications.

**Acknowledgment.** We thank Dr. Jacques Moser and Dr. Robin Humphry-Baker for helpful advice and discussions.

**Note Added after ASAP Publication:** This paper was published ASAP on March 5, 2008. The caption to Figure 2 was updated. The revised paper was reposted on March 22, 2008.

**Supporting Information Available:** Materials and methods. UV−vis curves of B1 in ethanol and adsorbed on an 8$\mu$ $TiO_2$ electrode. IR spectra of the solid dye powders of B1 in the acid form and in the form of the triethylammonium salt ($NEt_3$), as used in the dipping solution. IR spectra of B1 in the form of the acid and $NEt_3$ salt adsorbed on $TiO_2$, compared to the post-treatment of the latter, $NEt_3$ salt layer, with HCl. Structures of the organic dyes used by Bach to test the IPCE values both in the presence and absence of a compact layer. This material is available free of charge via the Internet at http://pubs.acs.org.

## References

(1) Jäger-Waldau, A.; Huld, T.; Šúri, M.; Cebecauer, T.; Dunlop, E.; Ossenbrink, H. *Conference Record of the 2006 IEEE 4th World Conference on Photovoltaic Energy Conversion*; IEEE: New York, 2006; Vol. 2, pp 2481–2484.
(2) Zweibel, K. *Thin Film Solar Cells* **2006**, *11*, 427.
(3) Schmidt-Mende, L.; Bach, U.; Humphry-Baker, R.; Horiuchi, T.; Miura, H.; Ito, S.; Uchida, S.; Grätzel, M. *Adv. Mater.* **2005**, *17*, 813.
(4) Horiuchi, T.; Miura, H.; Sumioka, K.; Uchida, S. *J. Am. Chem. Soc.* **2004**, *126*, 12218.
(5) Hara, K.; Kurashige, M.; Dan-oh, Y.; Kasada, C.; Shinpo, A.; Suga, S.; Sayamaa, K.; Arakawa, H. *New J. Chem.* **2003**, *27*, 783.
(6) Ito, S.; Liska, P.; Comte, P.; Charvet, R.; Pecchy, P.; Bach, U.; Schmidt-Mende, L.; Zakeeruddin, S.; Kay, A.; Nazeeruddin, M.; Grätzel, M. *Chem. Commun.* **2005**, *34*, 4351.
(7) Hagfeldt, A.; Grätzel, M. *Acc. Chem. Res.* **2000**, *33*, 269.
(8) Burke, A.; Schmidt-Mende, L.; Ito, S.; Grätzel, M. *Chem. Commun.* **2006**, *3*, 234.
(9) Ferber, J.; Stangl, R.; Luther, J. *Sol. Energy Mater. Sol. Cells* **1998**, *53*, 29.
(10) Nelson, J. *The Physics of Solar Cells*; Imperial College Press: London, 2003.
(11) O'Regan, B.; Lenzmann, F. *J. Phys. Chem. B* **2004**, *108*, 4342.
(12) Boschloo, G.; Goosens, A.; Schoonmann, J. *J. Electrochem. Soc.* **1997**, *144*, 1311.
(13) Nazeeruddin, M.; Humphry-Baker, R.; Liska, P.; Grätzel, M. *J. Phys. Chem. B* **2003**, *107*, 8981.
(14) Gude, C.; Rettig, W. *J. Phys. Chem. A* **2000**, *104*, 8050.
(15) Kobayashi, Y.; Goto, M.; Kurahashi, M. *Bull. Chem. Soc. Jpn.* **1986**, *59*, 311.
(16) Shklover, V.; Ovchinnikov, Yu.; Braginsky, L.; Zakeeruddin, S.; Graetzel, M *Chem. Mater.* **1998**, *10*, 2533.
(17) Ito, S.; Zakeeruddin, S.; Humphry-Baker, R.; Liska, P.; Charvet, R.; Comte, P.; Nazeeruddin, M.; Péchy, P.; Takata, M.; Miura, H.; Uchida, S.; Grätzel, M. *Adv. Mater.* **2006**, *18*, 1202.

NL071588B